

**Online Supplementary Material for**

**Targeting Negative Surface Charges of Cancer Cells by Multifunctional  
Nanoprobes**

Bingdi Chen, et al.

**Table S1 | List of cell lines used in the experiments shown in Fig. 5A**

Cell Line Names	Tissue Source	Species	Supplier
Hela	Cervical cancer	Human	SICB*
S180	Sarcoma	Mouse	SICB
K562	Leukemia	Human	SICB
HepG2	Liver cancer	Human	SICB
LM-3	Liver cancer	Human	Fudan University
SKOV-3	Ovarian cancer	Human	SICB
MCF-7	Breast cancer	Human	SICB
PC-3	Prostate cancer	Human	SICB
LNCaP	Prostate cancer	Human	SICB
HCT116	Colon cancer	Human	SICB
SW480	Colon cancer	Human	Fudan University
HGC-27	Gastric cancer	Human	SICB
BGC-823	Gastric cancer	Human	Fudan University
A549	Lung cancer	Human	SICB
F56	Gland cancer	Human	Fudan University
SW1990	Pancreatic cancer	Human	Changhai Hospital
BxPC-3	Pancreatic cancer	Human	Changhai Hospital
U87	glioma	Human	SICB
HuH-7	Liver cancer	Human	SICB
KB	Oral epidermoid carcinoma	Human	SICB
Caco-2	Colorectal adenocarcinoma	Human	SICB
CAL-27	Tongue squamous cell carcinoma	Human	SICB
PMN (Polymorphic nuclear cells)	Peripheral blood	Human	Healthy volunteer
MNC (mononuclear cells)	Peripheral blood	Human	Healthy volunteer
Hepatocytes	Liver	Rat	Primary cell Culture
Kidney cells	Kidney	Mouse	Primary cell Culture

\*SICB=Shanghai Institute of Cell Biology (China)

## Supplementary Figures

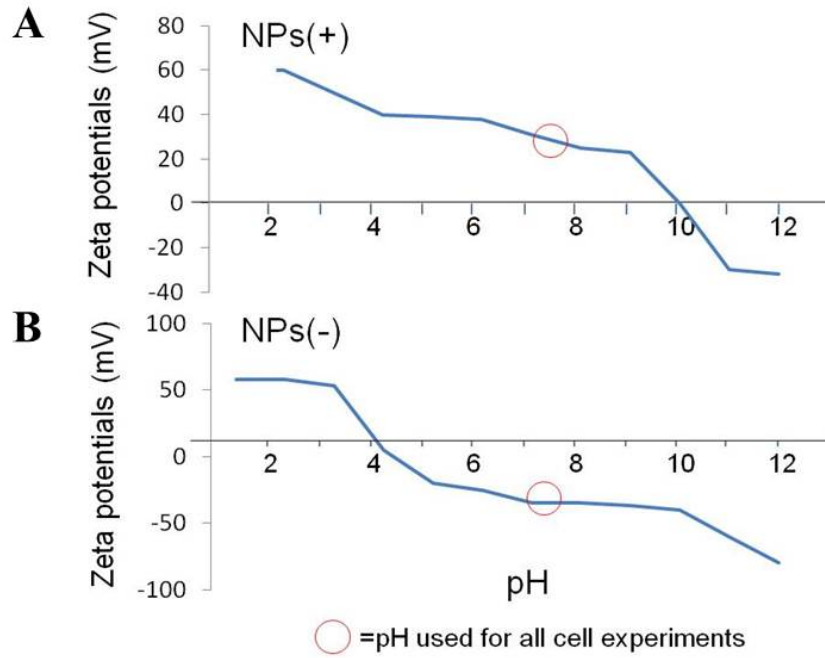


**Figure S1** Characterization of the paired NPs. (A) Zeta potential vs. pH for the positive NPs, and (B) Zeta potential vs. pH for the negative NPs. Note that the pH values for all cell experiments using the negative and positive NPs are marked by small circles.

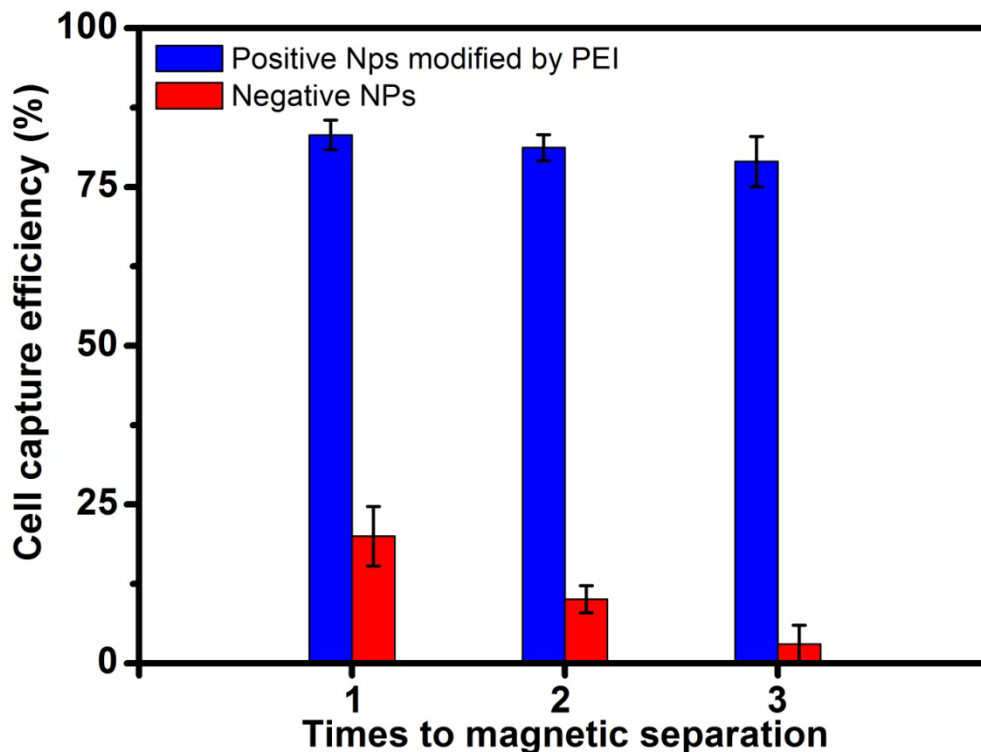


**Figure S2.** Effect of additional washes on the nonspecific binding of nanoprobes to cancer cells.

When a small portion of cancer cells bound to both positive and negative nanoprobes and captured, it seemed there might be a low level of nonspecific trapping of cells. In order to address this potential problem, we repeated the magnetic separation 2 times after resuspension in PBS (Figure S2). The results show that more than 85% of the bindings to the negative nanoprobes could be washed away, whereas the cells bound to the positive nanoprobes remained largely unchanged.

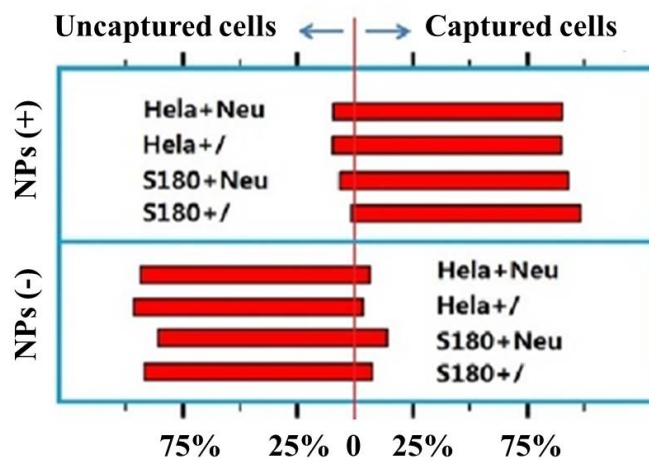


**Figure S3** Effect of saliva acid on cell surface on the percentages of cells captured by the positive and negative NPs. The magnetic capture efficiencies for both positive and negative NPs after the sialidase treatment. Neuraminidase (sialidase, 1.28 mg/ml) was added and co-incubated at 37°C for 30 min.

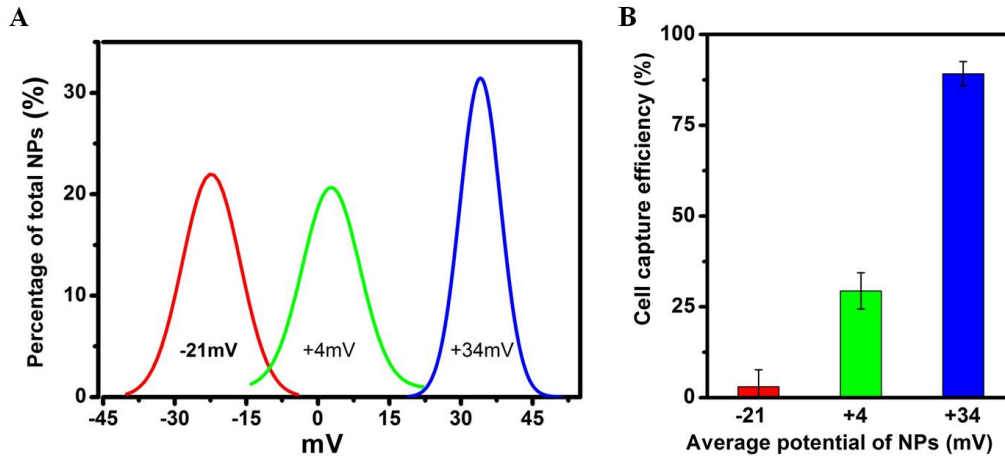


**Figure S4.** (A) Zeta potential distributions of NPs with average potentials of -21 mV, +4mV and +34 mV. (B) Magnetic capture efficiencies of K562 cells by three kinds of charge NPs.

To confirm that the efficiency of capture has a linear relationship with the level of positive charges on the nanoparticles, we created 3 different batches of nanoprobe with a gradient of average surface charges (Figure S4). The result shows that the capture efficiency of cancer cells is indeed proportional to level of surface positive charges.

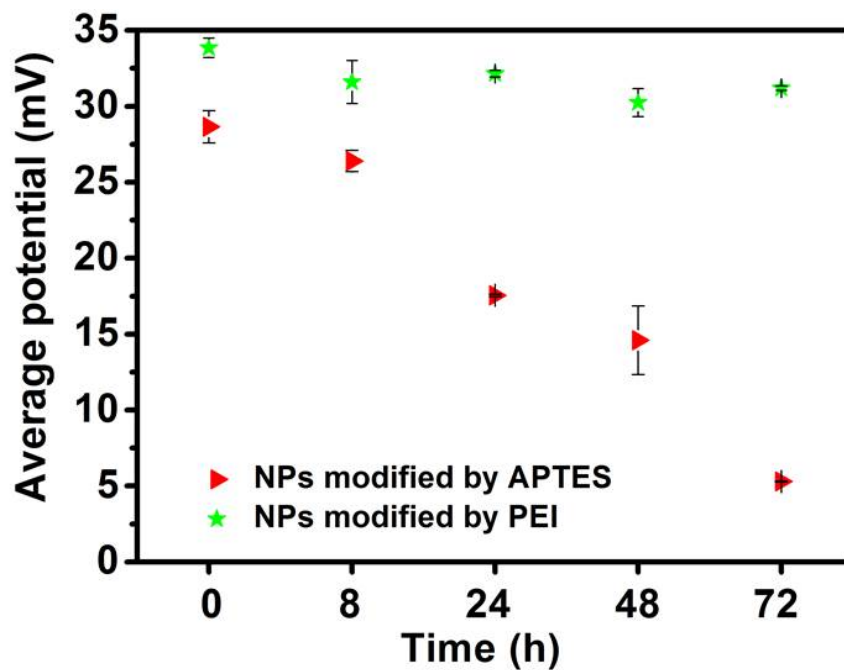


**Figure S5.** Different stabilities of the surface charges generated from PEI and APTES modification.

When we measured the average surface charges, it was apparent that the positive charges generated with PEI were stable for over 6 months, on the other hand, the positive charges generated with APTES were extremely unstable, more than 80% of the charges were lost within 72 hours (Figure S5).